Brief Reports

Brief Reports are accounts of completed research which, while meeting the usual **Physical Review** *standards of scientific quality, do not warrant regular articles. A Brief Report may be no longer than four printed pages and must be accompanied by an abstract. The same publication schedule as for regular articles is followed, and page proofs are sent to authors.*

Proton-glass behavior and phase diagram of the $K_{1-x}(NH_4)_xH_2PO_4$ system

Oh Jung Kwon and Jong-Jean Kim*

Physics Department, Korea Advanced Institute of Science and Technology, 373-1 Kusung-dong, Yusung-ku, Taejon 305-701, Korea

(Received 12 March 1993)

Both real and imaginary parts of the dielectric constants are measured in the pellet samples of $K_{1-x}(NH_4)_xH_2PO_4$ [$(KDP)_{1-x}(ADP)_x$ or KADP-x] for a full range of mixing concentrations x from $x=0$ to $x=1$ at temperatures from room temperature to 15 K. Both ferroelectric and antiferroelectric phase transitions are observed for $x<0.22$ and $x>0.70$, respectively, but proton-glass behaivor is observed in the range $0.28<x<0.64$ and phase coexistences are observed for x of the phase boundary layers in the pressed pellet samples of KADP-x. Observation of the proton-glass behavior in the mixed-pellet system of KADP-x, which consists of microcrystalline grains, seems to confirm that the proton-glass phase may originate from a strong frustration in the short-range pairing of hydrogen bonds associated with randomly competing site interactions.

I. INTRODUCTION

Mixed crystals of the KDP family between ferroelectric and antiferroelectric substances are found to exhibit a low-temperature glass phase in a certain range of mixing concentration characteristic of the mixing constituents.[1-4]

Both $Rb_{1-x}(NH_4)_xH_2PO_4$ (RADP-x) and $Rb_{1-x}(NH_4)_xH_2AsO_4$ (RADA-x) crystals can be grown in a full range of x and most previous research on the proton glass has been performed with these two systems.[4-9] The most well-known KDP family crystals, KH_2PO_4 (KDP) and $NH_4H_2PO_4$ (ADP), however, have been employed for proton-glass studies in a very limited range of mixing concentration x simply due to the extreme difficulty of mixed crystal growing caused by a large mismatch in lattice constants between KDP and ADP crystals. Previous proton-glass studies on the mixed crystals of $K_{1-x}(NH_4)_xH_2PO_4$ [$(KDP)_{1-x}(ADP)_x$ or KADP-x] have thus been limited to $x\leq 0.32$ and $x\geq 0.85$,[10-14] while pressed-pellet samples of KADP-x were studied to find the low-temperature proton-glass behavior at $x=0.5$.[15]

We have extended the pellet sample studies of the KADP-x system in the full range of mixing concentration from $x=0$ to 1. In addition to studying the x-T phase diagram of KADP-x it will be also interesting to compare the phase transition anomalies between single-crystal systems and powder pellet systems of KDP and ADP corresponding to $x=0$ and 1, respectively, and also the glass transition anomalies between the crystal and pellet samples in the glass-forming range of mixing concentration x.

II. EXPERIMENT

KADP-x powder was obtained by grinding the dried lump of polycrystalline aggregates precipitated from the homogeneous saturated solutions of KADP-x by the slow evaporation where KDP and ADP were mixed in the appropriate molar ratio x. Each KDP and ADP used was purified by recrystallization. The dried mixture was ground in a mortar and pressed under about 60 tons per square inch pressure to form pellets of 12.7 mm diameter and 0.6 mm thickness. Silver electrodes were vacuum coated on the pressed-pellet faces. Real (ϵ') and imaginary (ϵ'') parts of the dielectric constants were measured simultaneously in the frequency range of 1 kHz to 10 MHz by an impedance analyzer (HP4192A) at temperatures between 5 and 270 K. A closed-cycle helium refrigerator with a temperature control system (DRC-91CA, Lake Shore) was used for low-temperature controls of the sample with both cooling and heating rates at 0.5 K/min. A calibrated Si-diode sensor was used to measure the sample temperatures.

III. RESULTS AND DISCUSSION

In Fig. 1, we have shown the dielectric constants ϵ' and ϵ'' of pressed-pellet samples of KADP-x for $x=0$ and 0.1 observed as a function of temperature. The $x=0$ pellet sample shows the transition peak of the divergence anomaly as for the single-crystal KDP but with the peak value very much reduced for pellets. This reduction of the peak value may be attributed to the random orientations of crystallites in the pellet and finite-size effects[16] of each crystallite. The domain-wall contributions to the dielectric constant ϵ' in the ferroelectric phase are observed in the pellet sample as a shoulder anomaly extending to 60 K. The microcrystalline grains were observed to have a size distribution of about 1 μm in diameter as examined under the polarizing optical microscope, and these grains may still accommodate ferroelectric domain walls although the domain width is usually observed to be in the

range of 1–3 μm in the large single-crystal samples of KDP.[17] It reflects that the domain width D is dependent on temperature and also on the sample thickness t as $D \propto \sqrt{t}$.[18] At $x=0.06$ the dielectric constant ϵ' still shows a separate peak of the ferroelectric transition and the shoulder anomaly of the domain-wall contributions. The ferroelectric transition temperature was lowered, indicating the ammonium ion NH_4^+ to be effective as a hard defect in KDP with respect to the ferroelectric instability.

Further reduction in the transition peak values of the dielectric constant ϵ' may imply some ferroelectric bonds being frustrated by the antiferroelectric impurities of NH_4^+ ions in addition to the random orientations of the microcrystalline grains, where a-axis dielectric constants remain finite at the ferroelectric transition temperature T_c. As the mixing concentration x of the ammonium ion NH_4^+ is increased to $x=0.14$, the dielectric constant ϵ' shows one broad peak as often encountered in the diffused phase transition of the mixed crystal systems.[19,20] This feature continues to be observed at $x=0.22$ as shown in Fig. 2. At $x=0.28$ the Curie-Weiss law of the ferroelectric system is observed to break down well before reaching the maximum peak as can be seen in Fig. 3. This rounding off of the peak seems to be ascribed to the competing interactions marginal for both ferroelectric ordering and proton-glass random freezing. As the mixing concentration x is further increased to $x=0.5$ (see Fig. 3) we can observe the typical dielectric constant curve of the proton-glass transition: deviation of the Curie-Weiss law at a relatively well-defined onset temperature of local freezing followed by a plateau region of fixation and then a sharp falloff of the glass phase transition. Furthermore, a significant frequency dependence of the glass transition temperature T_g corresponding to the dielectric loss peak also confirms the proton-glass phase in KADP-x for $x=0.57$ as observed in Fig. 3(c).

Further increase of x to $x=0.64$ seems to drive the KADP-x system towards the antiferroelectric side but competing with the proton-glass formation. Coexistence clusters of frustrated dipoles randomly mixed with the antiferroelectric domains seems to go ultimately into

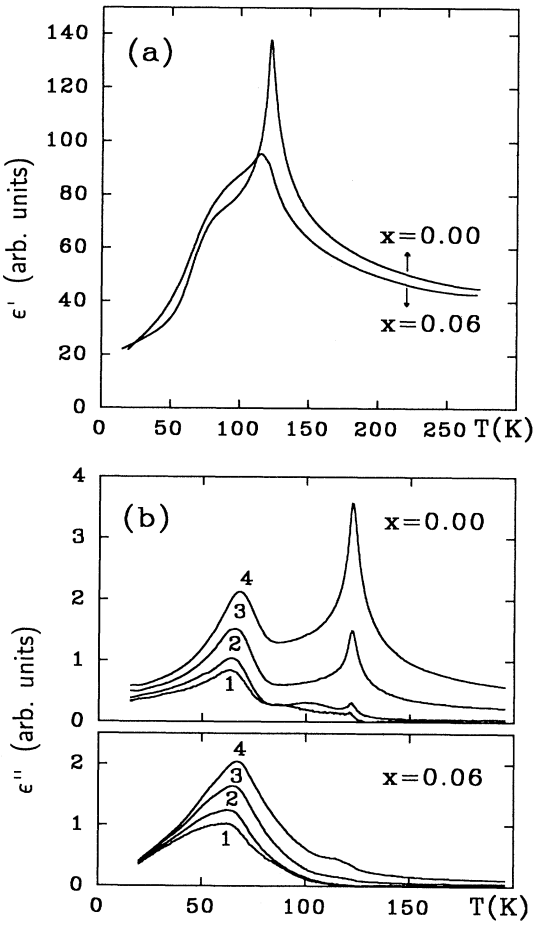

FIG. 1. Temperature dependence of dielectric constants ϵ' and ϵ'' in KADP-x pellets: (a) Real part ϵ' for $x=0.0$ and 0.06 as measured at $\omega=12$ kHz. (b) Imaginary parts ϵ'' for $x=0.0$ (upper ones) and $x=0.06$ (lower ones) as measured at varying frequencies of (1) $\omega=12$ kHz, (2) $\omega=87.7$ kHz, (3) $\omega=640$ kHz, and (4) $\omega=1.73$ MHz.

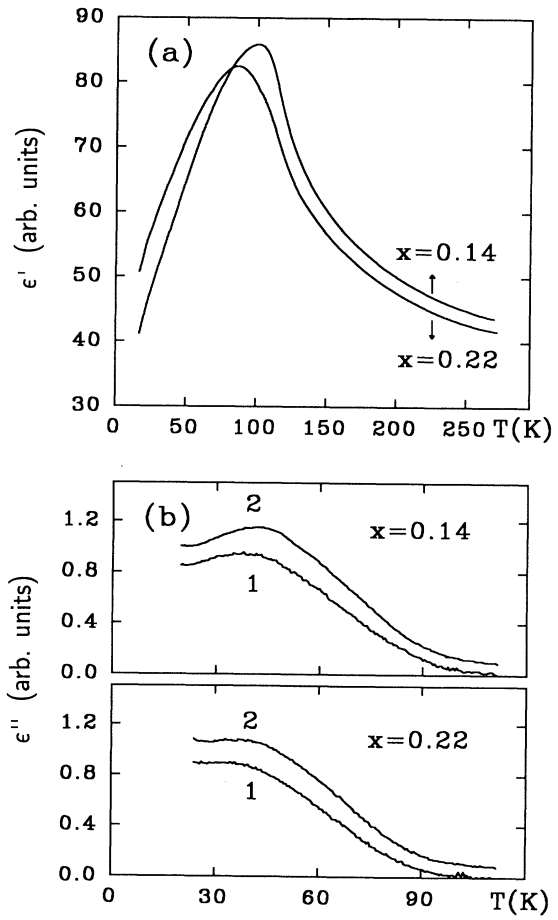

FIG. 2. Temperature dependence of dielectric constants ϵ' and ϵ'' in KADP-x pellets: (a) Real part ϵ' for $x=0.14$ and 0.22 as measured at $\omega=12$ kHz. (b) Imaginary part ϵ'' for $x=0.14$ (upper ones) and $x=0.22$ (lower ones) as measured at frequencies of (1) $\omega=12$ kHz, and (2) $\omega=87.7$ kHz.

complete freezing at the glass transition temperature as can be seen in Fig. 4. As the ammonium-ion concentration x is increased to above $x=0.70$ (see Figs. 4 and 5), the frustration may no longer be strong enough to prevent the long-range-ordered antiferroelectric ground state in the KADP-x system as can be seen from Fig. 5.

We also see a large downward shift of the antiferroelectric transition temperature T_N in KADP-x for $x=0.81$, indicating KDP impurities also playing a hard defect role in ADP crystal. The $x=1.0$ sample, corresponding to pure ADP, can be seen to be free from the shattering problem of the ADP single crystal at the antiferroelectric transition point.

In Fig. 6, we show the x-T phase diagram of the KADP-x system as obtained from the dielectric measurements on the pellet samples. Both ferroelectric and antiferroelectric transition temperatures are determined as corresponding to the maximum peak temperatures of ϵ'

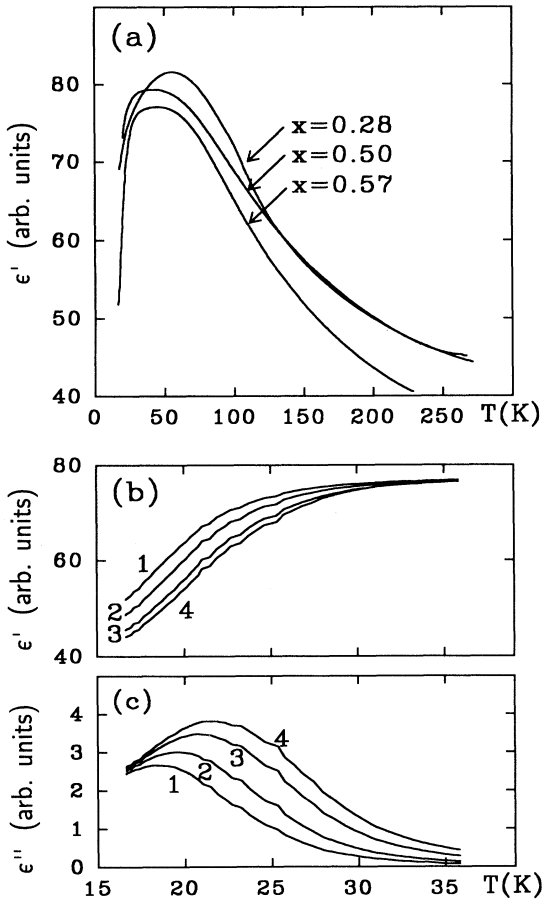

FIG. 3. Temperature dependence of dielectric constants ϵ' and ϵ'' in KADP-x pellets: (a) Real part ϵ' for $x=0.28$, 0.50, and 0.57 as measured at $\omega=12$ kHz. (b) Frequency dispersion of ϵ' observed with KADP-x ($x=0.57$) at low temperatures below 35 K: (1) $\omega=12$ kHz, and (2) $\omega=87.7$ kHz, (3) $\omega=640$ kHz, and (4) $\omega=1.73$ MHz. (c) Frequency dispersion of ϵ'' observed with KADP-x ($x=0.57$) at low temperatures below 35 K: (1) $\omega=12$ kHz, (2) $\omega=87.7$ kHz, (3) $\omega=640$ kHz, and (4) $\omega=1.73$ MHz.

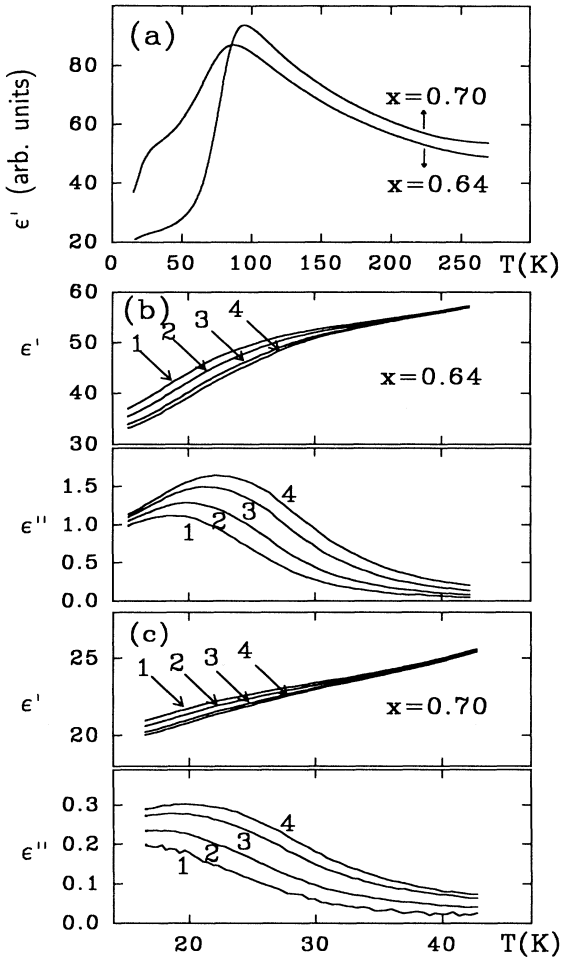

FIG. 4. Temperature dependence of dielectric constants ϵ' and ϵ'' in KADP-x pellets: (a) Real part ϵ' for $x=0.64$ and 0.70 as measured at $\omega=12$ kHz. (b) Frequency dependence of ϵ' and ϵ'' observed with KADP-x ($x=0.64$) at low temperatures below 40 K: (1) $\omega=12$ kHz, (2) $\omega=87.7$ kHz, (3) $\omega=640$ kHz, and (4) $\omega=1.73$ MHz. (c) Frequency dependence of ϵ' and ϵ'' in KADP-x ($x=0.70$) at low temperatures below 40 K: (1) $\omega=12$ kHz, (2) $\omega=87.7$ kHz, (3) $\omega=640$ kHz, and (4) $\omega=1.73$ MHz.

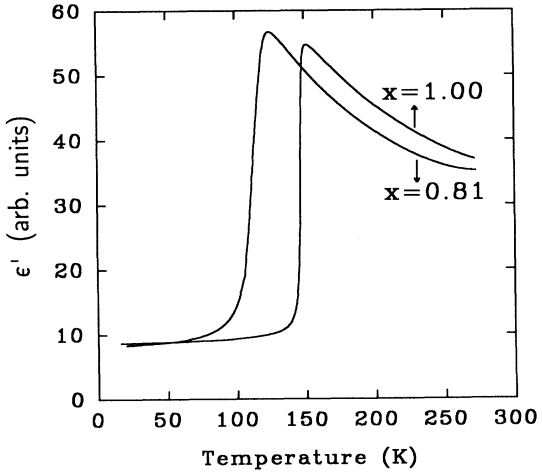

FIG. 5. Temperature dependence of dielectric constants ϵ' in KADP-x pellets for $x=0.81$ and 1.0.

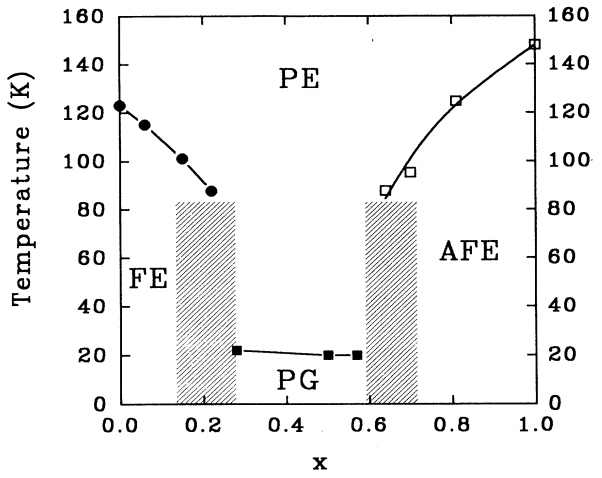

FIG. 6. x-T phase diagram in the KADP-x system: FE for ferroelectric, PE for paraelectric, AFE for antiferroelectric, and PG for proton-glass phase, respectively, shaded columns represent regions of a possible two-phase coexistence.

while the proton-glass transition temperatures are defined as corresponding to the points of falloff from the plateau of the dielectric constant ϵ'. Frequency dispersions of dielectric constants ϵ' and ϵ'' as observed in Figs. 3(b), 3(c), and 4(b) also help to confirm the glass transitions and to locate the glass transition temperature as corresponding to the loss peaks at around 20 K.

IV. CONCLUSION

With pellet samples of $K_{1-x}(NH_4)_xH_2PO_4$ (KADP-x) we could obtain the x-T phase diagram of KADP-x $[(KDP)_{1-x}(ADP)_x]$ over the full range of mixing concentration x. Random orientations of the microcrystallites and finite-size effects of each microcrystallite do not seem to give serious effects on the proton-glass formation to bring a qualitative change in the phase diagram between single-crystal and pellet samples of KADP-x. In other words, KADP-x pellet samples are as good as the single-crystal samples for dielectric studies of the proton-glass behavior in KADP-x systems unless we have problems of anisotropy in the glass phase order parameter or critical fluctuations of long-range ordering with correlation length well over the grain size, especially in the two-phase coexistence region where short-range clustering is randomly competing with long-range ordering.

ACKNOWLEDGMENTS

This work was supported in part by the Korea Science and Engineering Foundation (RCDAMP-1992).

*Author to whom correspondence should be addressed.

[1]E. Courten, J. Phys. (Paris) **43**, L199 (1983).
[2]S. Iida and H. Terauchi, J. Phys. Soc. Jpn. **52**, 4044 (1983).
[3]Z. Trybula, J. Stankowski, and R. Blinc, Ferroelectrics Lett. **6**, 57 (1986).
[4]Z. Trybula, V. H. Schmidt, J. E. Drumheller, and R. Blinc, Phys. Rev. B **42**, 6733 (1990).
[5]E. Courtens, Ferroelectrics **72**, 229 (1987).
[6]Z. Trybula, V. H. Schmidt, and J. E. Drumheller, Phys. Rev. B **43**, 1287 (1991).
[7]J. Eom, J. Yoon, and S. I. Kwun, Phys. Rev. B **44**, 2826 (1991).
[8]A. Levstik, C. Filipic, Z. Kutnjak, I. Levstik, R. Pirc, B. Tadic, and R. Blinc, Phys. Rev. Lett. **66**, 2368 (1991).
[9]J.-J. Kim and H. G. Shin, Ferroelectrics **135**, 319 (1992).
[10]Y. Ono, T. Hikita, and T. Ikeda, J. Phys. Soc. Jpn. **56**, 577 (1987).
[11]S. A. Grdnev, L. N. Korotkov, and S. P. Rogova, Ferroelectrics Lett. **13**, 67 (1991).
[12]M. Vaezzadeh, B. Wyncke, and F. Bréhat, J. Phys. Condens. Matter **4**, 7401 (1992).
[13]B. Wyncke, F. Bréhat, and M. Vaezzadeh, Ferroelectrics **107**, 139 (1990).
[14]Y. Ono, T. Hikita, and T. Ikeda, Ferroelectrics **79**, 327 (1988).
[15]J.-J. Kim and W. F. Sherman, Phys. Rev. B **36**, 5651 (1987).
[16]H. E. Müser and R. Siems, Jpn. J. Appl. Phys. **24**, 195 (1985).
[17]D. H. Ha and J.-J. Kim, Jpn. J. Appl. Phys. **24**, 556 (1985).
[18]T. Mitsui and J. Furuichi, Phys. Rev. **90**, 193 (1953).
[19]A. M. Glass, J. Appl. Phys. **40**, 4699 (1969).
[20]M. E. Lines and A. M. Glass, *Principles and Applications of Ferroelectrics and Related Materials* (Oxford University Press, Oxford, 1977), p. 285.